Proceedings of 2018 ISFA
2018 International Symposium on Flexible Automation
Kanazawa, Japan, 15 - 19 July, 2018

(ISFA2018-L096)

A LIFTED DOMAIN-BASED METRIC FOR PERFORMANCE EVALUATION OF LTI AND LTV DISCRETE-TIME TRACKING CONTROLLERS

Keval S. Ramani
Department of Mechanical Engineering
University of Michigan
Ann Arbor, MI, 48109
ksramani@umich.edu

Molong Duan
Department of Mechanical Engineering
University of Michigan
Ann Arbor, MI, 48109
molong@umich.edu

Chinedum E. Okwudire
Department of Mechanical Engineering
University of Michigan
Ann Arbor, MI, 48109
okwudire@umich.edu

A. Galip Ulsoy
Department of Mechanical Engineering
University of Michigan
Ann Arbor, MI, 48109
ulsoy@umich.edu

ABSTRACT

The Frobenius norm of the lifted system representation of tracking error dynamics is proposed as a metric for evaluating the tracking performance of discrete-time linear time invariant (LTI) and linear time varying (LTV) controllers. The proposed metric is introduced here in the context of feedforward tracking control of LTI single-input single-output (SISO) nonminimum phase (NMP) systems, though it is more broadly applicable. It is shown that the filtered basis functions (FBF) approach, an LTV tracking control technique studied by the authors in prior work, is the optimal solution to the rank constrained minimization of the proposed metric. Moreover, for the FBF controller, the metric is independent of plant dynamics, which is not the case for most other tracking controllers; it is also independent of the type of basis functions employed in the FBF controller. The effectiveness of the proposed metric as a tracking performance evaluation tool for both LTI and LTV tracking controllers is demonstrated analytically and numerically on LTI plants with different zero locations.

NOMENCLATURE

Symbol	Description
A	Exponential function constant
C	Feedforward controller
$\mathbf{C}$	Lifted system representation of feedforward controller
E_{ff}	Error dynamics
$\mathbf{E}_{ff}$	Lifted system representation of error dynamics
G	Plant
$\mathbf{G}$	Lifted system representation of plant
$\mathbf{I}$	Identity matrix
J_e	Proposed Frobenius norm metric for tracking error
L	Overall dynamics
$\mathbf{L}$	Lifted system representation of overall dynamics
M	Number of trajectory points minus 1
a	Zero location
e	Tracking error
$\mathbf{e}$	Lifted form of tracking error
j	Unit imaginary number
k	Discrete time index
n	Number of basis functions minus 1
n_1	Number of terms used in truncated series method
p	Pole location
q	Forward shift operator
u	Control input
$\mathbf{u}$	Lifted form of control input
y	Output
$\mathbf{y}$	Lifted form of output
y_d	Desired trajectory
$\mathbf{y}_d$	Lifted form of desired trajectory
$\mathbf{\Phi}$	Basis function matrix
$\mathbf{\Psi}$	Basis function matrix corresponding to decoupled filtered basis functions
$\boldsymbol{\alpha}$	Transformation matrix
β_i	Constant factor for DCT basis functions
γ_i	Coefficients of basis functions
$\boldsymbol{\gamma}$	Vector representation of coefficients
$\boldsymbol{\eta}_i$	Singular vectors of identity matrix
μ	Exponential function constant
σ_i	Singular values of $\mathbf{E}_{ff}$
φ_i	Basis functions
$\boldsymbol{\varphi}_i$	Lifted form of basis functions
~	Filtered variable
*	Optimal variable

1. INTRODUCTION

Tracking control is a fundamental problem encountered in a wide range of fields such as manufacturing, robotics and aeronautics. The objective of tracking control is to force the output trajectory of the controlled system to follow a desired trajectory as closely as possible. Tracking control could be achieved using feedforward and/or feedback controllers. This paper is written in the context of feedforward tracking control of discrete-time, linear time-invariant (LTI), single-input single-output (SISO), nonminimum phase (NMP) systems. However, its key results apply to any discrete-time linear tracking controller, whether feedforward or feedback, time invariant or time varying.

Discrete-time feedforward tracking techniques for SISO LTI systems usually result in LTI controllers, e.g., zero phase error tracking control [1], truncated series [2], and others (see [3–7] for more details). However, there are a few techniques that can result in linear time varying (LTV) controllers [7–10]. For instance, perfect tracking control can be achieved using the lifted system representation of an LTI system [3]. However, for NMP systems, the lifted representation has small singular values which prevent inversion. Hence, Hashemi and Hammond [8] proposed a small singular values substitution method which generally results in an LTV controller. Similarly, to address the same problem, Ronde et al. [9] used a truncated SVD (singular value decomposition) approach which also results in an LTV controller. Norm optimal iterative learning control [7], an optimization based tracking control technique, can also result in an LTV controller.

The filtered basis functions (FBF) method is another class of tracking controllers that is LTV [10–12]. It finds its origins in the work of Frueh and Phan [13] on inverse linear quadratic learning in the context of iterative learning control (ILC). The FBF approach expresses the control input as a linear combination of user-defined basis functions with unknown coefficients. The basis functions are forward filtered using the plant dynamics, and their coefficients selected such that the tracking error is minimized. Unlike comparable methods in the literature, the present authors have shown that the FBF method is effective in tracking any desired trajectory, irrespective of the location of NMP zeros in the z-plane – including nonhyperbolic systems [10,11]. Moreover, using time-domain simulation examples, they have shown that the FBF method maintains consistent tracking performance compared to popular LTI tracking controllers irrespective of the location of NMP zeros in the z-plane. However, while the use of time-domain simulation examples [3,4,10] and cost functions based on signal 2-norms [7,14] is common for evaluating tracking controllers, such evaluations often depend on specific desired trajectories, and hence could lack generality and fundamental insight. This drawback of time-domain-based evaluation is often overcome in LTI controllers by employing frequency domain metrics like Bode diagrams [2], transfer function magnitude at Nyquist frequency [4], and system 2-norms [2,3], etc. However, such frequency-domain metrics do not generally apply to LTV controllers. It is therefore desirable to develop metrics that are suitable for tracking performance evaluation of LTV controllers (in comparison with their LTI counterparts), independent of specific desired trajectories.

For discrete-time tracking controllers, the lifted domain provides a unified framework for representing both LTI and LTV tracking controllers [7]. Therefore, it makes sense to explore a unified metric for tracking error evaluation for LTI and LTV controller using the lifted domain representation. In this regard, the 2-norm of the lifted system representation of controlled systems has been used for evaluating the convergence of tracking errors (i.e., stability analysis) in ILC, independent of specific desired trajectories [15]. However, as discussed in Sec. 3.2, the use of the 2-norm of lifted system representation can be misleading for tracking performance evaluation of controllers. This paper makes the following key contributions to the literature to address the aforementioned shortcomings:

1. It proposes the Frobenius norm of the lifted system representation of tracking error dynamics as a metric for evaluating the tracking performance of LTI and LTV controllers, independent of desired trajectory (Sec. 2).
2. It shows that the FBF controller is the optimal solution to the rank constrained minimization of the proposed Frobenius norm metric. It also shows analytically that, for the FBF controller, the metric is independent of plant dynamics (and of the choice of basis functions) (Sec. 3).
3. It analytically and numerically demonstrates the effectiveness of the proposed metric as a tracking performance evaluation tool using LTI plants with different zero locations. Specifically, the Frobenius norm metric and time-domain tracking performances of the FBF (LTV) controller are compared to those of two popular LTI tracking controllers – namely, the zero phase error tracking controller and the truncated series controller (Sec. 4).

2. PROBLEM STATEMENT AND FROBENIUS NORM METRIC

2.1 Problem Statement

Given a discrete-time LTI SISO plant $G(q)$, as shown in Fig. 1, which may represent an open loop plant or a closed loop controlled system, we can write

$$y(k) = G(q)u(k) \tag{1}$$

where k is the time index, q is the forward shift operator, y and u are the output and control input, respectively. The objective of feedforward tracking control is to design a controller $C(q)$ or find a control input $u(k)$ given by

$$u(k) = C(q)y_d(k) \tag{2}$$

where $y_d(k)$ is the desired trajectory, such that the tracking error $e(k)$

$$\begin{aligned} e(k) &= y_d(k) - y(k) \\ &= (1 - \underbrace{G(q)C(q)}_{L(q)})y_d(k) = E_{ff}(q)y_d(k) \end{aligned} \tag{3}$$

is minimized, where $L(q)$ and $E_{ff}(q)$ are the overall and the error dynamics of the controlled system, respectively.

For finite time, $0 \le k \le M$ (M+1 is the number of discrete points in the trajectory), the desired trajectory, control input, tracking error and output trajectory can be expressed using vectors

$$\begin{aligned} \mathbf{y}_d &= \begin{bmatrix} y_d(0) & y_d(1) & \dots & y_d(M) \end{bmatrix}^{\mathrm{T}}, \\ \mathbf{u} &= \begin{bmatrix} u(0) & u(1) & \dots & u(M) \end{bmatrix}^{\mathrm{T}}, \\ \mathbf{e} &= \begin{bmatrix} e(0) & e(1) & \dots & e(M) \end{bmatrix}^{\mathrm{T}}, \\ \mathbf{y} &= \begin{bmatrix} y(0) & y(1) & \dots & y(M) \end{bmatrix}^{\mathrm{T}} \end{aligned} \tag{4}$$

Accordingly, Eqs. (1)-(3) can be expressed as

$$\mathbf{y} = \mathbf{G}\mathbf{u}; \quad \mathbf{u} = \mathbf{C}\mathbf{y}_d; \quad \mathbf{e} = \underbrace{(\mathbf{I} - \mathbf{L})}_{\mathbf{E}_{ff}}\mathbf{y}_d \tag{5}$$

where $\mathbf{G}$, $\mathbf{C}$, $\mathbf{L}$ and $\mathbf{E}_{ff}$ are the lifted system representations (see Appendix A for details) of G, C, L and E_{ff}, respectively, and $\mathbf{I}$ is the identity matrix of appropriate size.

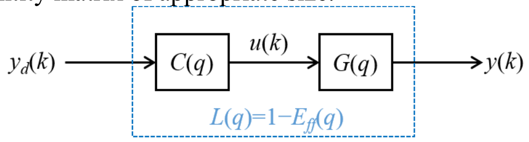

Figure 1: Block diagram for feedforward tracking control

2.2 Frobenius Norm Metric

As a tracking performance evaluation metric, this paper proposes the following metric, J_e, based on the Frobenius norm of $\mathbf{E}_{ff}$

$$J_e = \frac{\left\|\mathbf{E}_{ff}\right\|_F}{\sqrt{M+1}} \tag{6}$$

where

$$\left\|\mathbf{E}_{ff}\right\|_F = \sqrt{trace(\mathbf{E}_{ff}^{\mathrm{T}}\mathbf{E}_{ff})} = \sqrt{\sum_{\forall i}\left\{\sigma_i(\mathbf{E}_{ff})\right\}^2} \tag{7}$$

The Frobenius norm is selected because it takes into account all singular values/gains (σ_i) of $\mathbf{E}_{ff}$, as opposed to $\|\mathbf{E}_{ff}\|_2$, which considers only the maximum singular value/gain. The square root of (M+1) in the metric ensures that the metric is uniformly bounded as the length of the trajectory grows.

Note that for a normalized desired trajectory ($\|\mathbf{y}_d\|_2 = 1$),

$$\mathbf{e}_{RMS} = \frac{\|\mathbf{e}\|_2}{\sqrt{M+1}} \le \frac{\left\|\mathbf{E}_{ff}\right\|_F}{\sqrt{M+1}} = J_e \tag{8}$$

The implication is that J_e is an upper bound on the RMS tracking error ($\mathbf{e}_{RMS}$). Moreover, it is shown in Appendix B, that for an LTI system

$$\frac{\left\|\mathbf{E}_{ff}\right\|_F}{\sqrt{M+1}} \to \left\|E_{ff}(q)\right\|_2 \quad \text{as } M \to \infty \tag{9}$$

In other words, J_e approaches the system error 2-norm criterion (sometimes used in the design and analysis of LTI tracking controllers [2]) for large M.

Remark 1: The lifted system representation is employed for the proposed metric because it applies to both LTI and LTV controllers [7]. Moreover, the lifted system representation is applicable to feedforward as well as feedback controllers, SISO as well as multi-input multi-output (MIMO) controllers. As a result, the proposed metric is broadly applicable to any linear, discrete-time tracking controller.

3. FROBENIUS NORM METRIC APPLIED TO FILTERED BASIS FUNCTIONS APPROACH

Ideally, the feedforward tracking controller should be selected such that $C(q) = G(q)^{-1}$ ($\mathbf{C} = \mathbf{G}^{-1}$) which results in $E_{ff}(q) = 0$ ($\mathbf{E}_{ff} = \mathbf{0}$) and the proposed metric $J_e = 0$. However, $C(q) = G(q)^{-1}$ is unrealizable if $G(q)$ contains uncancellable zero(s). The presence of uncancellable zeros has motivated a lot of research (see [3–6,10] for more details). As mentioned in Sec.1, using time-domain simulation examples, the authors have shown that the filtered basis functions (FBF) method maintains consistent tracking performance compared to popular LTI tracking controllers irrespective of the location of NMP zeros in the z-plane [10,11,16]. However, due to lack of a suitable metric, the FBF method's tracking performance has not been evaluated independent of specific desired trajectories. This section presents an overview of the FBF approach and uses the proposed Frobenius norm metric to provide a theoretical justification for its observed consistent tracking performance.

3.1 Overview of FBF Approach

The FBF approach relies on two assumptions:

- the desired trajectory, y_d, is known *a priori*
- the control input $u(k)$ is expressed as a linear combination of n+1 user-defined basis functions $\varphi_i(k)$

$$u(k) = \sum_{i=0}^{n}\gamma_i\varphi_i(k) \tag{10}$$

where γ_i are unknown coefficients. Using vectors, Eq. (10) can be expressed as

$$\mathbf{u} = \mathbf{\Phi}\boldsymbol{\gamma} \tag{11}$$

where

$$\begin{gathered}\mathbf{\Phi} = \begin{bmatrix}\boldsymbol{\varphi}_0 & \boldsymbol{\varphi}_1 & \cdots & \boldsymbol{\varphi}_n\end{bmatrix}, \\ \boldsymbol{\varphi}_i = \begin{bmatrix}\varphi_i(0) & \varphi_i(1) & \cdots & \varphi_i(M)\end{bmatrix}^{\mathrm{T}}, \\ \boldsymbol{\gamma} = \begin{bmatrix}\gamma_0 & \gamma_1 & \cdots & \gamma_n\end{bmatrix}^{\mathrm{T}}\end{gathered} \tag{12}$$

For a linear system $G(q)$ (with lifted system representation $\mathbf{G}$), $\mathbf{y}$ can be expressed as

$$\mathbf{y} = \tilde{\mathbf{\Phi}}\boldsymbol{\gamma} \tag{13}$$

where

$$\begin{gathered}\tilde{\mathbf{\Phi}} = \mathbf{G}\mathbf{\Phi}; \quad \tilde{\boldsymbol{\varphi}}_i = \mathbf{G}\boldsymbol{\varphi}_i; \\ \tilde{\mathbf{\Phi}} = \begin{bmatrix}\tilde{\boldsymbol{\varphi}}_0 & \tilde{\boldsymbol{\varphi}}_1 & \cdots & \tilde{\boldsymbol{\varphi}}_n\end{bmatrix}\end{gathered} \tag{14}$$

represent the filtered basis functions. The control objective is to find the optimal coefficient vector $\boldsymbol{\gamma}$ such that the squared 2-norm of the tracking error

$$\mathbf{e}^{\mathrm{T}}\mathbf{e} = (\mathbf{y}_d - \tilde{\mathbf{\Phi}}\boldsymbol{\gamma})^{\mathrm{T}}(\mathbf{y}_d - \tilde{\mathbf{\Phi}}\boldsymbol{\gamma}) \tag{15}$$

is minimized; the optimal solution is given by

$$\boldsymbol{\gamma}^* = \left(\tilde{\mathbf{\Phi}}^{\mathrm{T}}\tilde{\mathbf{\Phi}}\right)^{-1}\tilde{\mathbf{\Phi}}^{\mathrm{T}}\mathbf{y}_d \tag{16}$$

Based on Eqs. (5), (11), (13) and (16), the lifted system representations of the controller and error dynamics of the FBF method can be expressed as

$$\begin{gathered}\mathbf{C}_{FBF} = \mathbf{\Phi}\left(\tilde{\mathbf{\Phi}}^{\mathrm{T}}\tilde{\mathbf{\Phi}}\right)^{-1}\tilde{\mathbf{\Phi}}^{\mathrm{T}} \\ \mathbf{E}_{ff,FBF} = \mathbf{I} - \underbrace{\tilde{\mathbf{\Phi}}\left(\tilde{\mathbf{\Phi}}^{\mathrm{T}}\tilde{\mathbf{\Phi}}\right)^{-1}\tilde{\mathbf{\Phi}}^{\mathrm{T}}}_{\mathbf{L}_{FBF}}\end{gathered} \tag{17}$$

The filtered basis functions matrix $\tilde{\mathbf{\Phi}}$ can be transformed to decoupled filtered basis functions $\tilde{\mathbf{\Psi}}$ using transformation $\boldsymbol{\alpha}$ (for more details, see prior work of the authors [10])

$$\begin{gathered}\tilde{\mathbf{\Phi}} = \tilde{\mathbf{\Psi}}\boldsymbol{\alpha} \\ \mathbf{\Phi} = \mathbf{\Psi}\boldsymbol{\alpha}\end{gathered} \tag{18}$$

such that

$$\tilde{\boldsymbol{\Psi}}^{\mathrm{T}}\tilde{\boldsymbol{\Psi}} = \mathbf{I} \tag{19}$$

and

$$\begin{aligned} \mathbf{C}_{FBF} &= \boldsymbol{\Psi}\tilde{\boldsymbol{\Psi}}^{\mathrm{T}} \\ \mathbf{E}_{ff,FBF} &= \mathbf{I} - \tilde{\boldsymbol{\Psi}}\tilde{\boldsymbol{\Psi}}^{\mathrm{T}} \end{aligned} \tag{20}$$

Remark 2: $\mathbf{C}_{FBF}$ and $\mathbf{E}_{ff,FBF}$ both depend on the plant as well as the selected basis functions. Both matrices are, in general, non-Toeplitz and non-triangular implying that the FBF controller is, in general, LTV and non-causal [10].

Remark 3: Although, this paper describes the FBF approach in the context of LTI SISO systems, it is applicable to other types of linear systems such as LTV and MIMO systems. Ref. [16] relaxes the assumption on *a priori* knowledge of the desired trajectory using B-spline basis functions.

3.2 Analysis of FBF using Proposed Frobenius Norm Metric

According to the Eckart−Young−Mirsky (EYM) Theorem [17–19], FBF is the optimal solution to the rank constrained minimization of the proposed Frobenius norm metric (for proof see Appendix C); i.e.,

$$\mathbf{L}_{FBF} := \arg\min_{\mathbf{L}} \left(J_e = \frac{\|\mathbf{I}-\mathbf{L}\|_F}{\sqrt{M+1}} \right) \quad \text{s.t. } rank(\mathbf{L}) \le n+1 \tag{21}$$

Remark 4: As discussed previously, $J_e = 0$ implies $\mathbf{C} = \mathbf{G}^{-1}$ which might be undesirable if $G(q)$ contains uncancellable zero(s) because such zeros result in very small singular values of **G,** and consequently large control signals [3]. The use of $n+1 < M+1$ basis functions imposes a rank constraint on $\mathbf{L}_{FBF}$ which in the lifted domain represents a restricted space of inputs and outputs [10]. The rank constraint avoids inversion of the full **G**, while also reducing the computational demands of the control problem [20–22].

Applying the proposed Frobenius norm metric to the FBF method yields

$$J_{e,FBF} = \sqrt{1-\frac{n+1}{M+1}} \tag{22}$$

This result stems from the fact that $\mathbf{E}_{ff,FBF}$ is symmetric, idempotent and has $M-n$ singular values equal to 1. Note that $J_{e,FBF}$ is independent of the plant ($G(q)$) and the type of basis functions employed. It depends only on the number of basis functions and the number of discrete points in the trajectory. As will be shown in the following section, the independence of $J_{e,FBF}$ from $G(q)$ cannot be taken for granted with other tracking controllers; it stems from the unique structure of $\mathbf{E}_{ff,FBF}$ and it explains the consistent tracking performance of the FBF method irrespective of $G(q)$, as observed in prior work [10,11,16]. Note that, $\|\mathbf{E}_{ff,FBF}\|_2$ is equal to 1, irrespective of the number of basis functions used, which is not a realistic representation of the tracking performance of the FBF method, which varies significantly with n [10,11,16]. Hence, the proposed Frobenius norm metric is more appropriate compared to 2-norm metrics like those used in ILC [15].

4. VALIDATION OF THE FROBENIUS NORM METRIC

To demonstrate the effectiveness of the proposed metric, this section compares the J_e value and tracking performance of FBF with those of the Zero Phase Error Tracking Controller (ZPETC) and Truncated Series (TS) tracking controllers using a first order plant studied by Butterworth et al. [4]:

$$G(q) = \frac{q-a}{q-p} \tag{23}$$

where a (a real number) and $p = 0.5$ are the zero and pole of the plant, respectively. The ZPETC [1] is a widely discussed technique in the literature, and TS [2] is the optimal solution to the constrained minimization of weighted integral of squared magnitude of the error dynamics; it is one of the most versatile controllers with regards to its ability to deliver excellent tracking irrespective of the plant dynamics.

As shown in the preceding section, the Frobenius norm metric J_e for FBF is independent of the plant dynamics (see Eq. (22)). For ZPETC, the error dynamics $E_{ff}(q)$ and metric J_e are given by

$$\left.\begin{aligned} L_{ZPETC}(q) &= \frac{(q-a)(q^{-1}-a)}{(1-a)^2} \\ \Rightarrow E_{ff,ZPETC}(q) &= \frac{aq^{-1}-2a+aq}{(1-a)^2} \\ \Rightarrow J_{e,ZPETC} &= \sqrt{6-\frac{2}{M+1}}\frac{|a|}{(1-a)^2} \end{aligned}\right\} a \ne 1 \tag{24}$$

For TS, the expressions are given by

$$\begin{aligned} L_{TS}(q) &= \begin{cases} 1-a^{-n_1}q^{n_1} & |a|>1 \\ 1-a^{n_1}q^{-n_1} & |a|<1 \end{cases} \\ \Rightarrow E_{ff,TS}(q) &= \begin{cases} a^{-n_1}q^{n_1} & |a|>1 \\ a^{n_1}q^{-n_1} & |a|<1 \end{cases} \\ \Rightarrow J_{e,TS} &= \begin{cases} \sqrt{1-\frac{n_1}{M+1}}|a|^{-n_1} & |a|>1 \\ \sqrt{1-\frac{n_1}{M+1}}|a|^{n_1} & |a|<1 \end{cases} \end{aligned} \tag{25}$$

where n_1 is the number of terms in the series.

Remark 5: The expressions of J_e for ZPETC and TS given by Eqs. (24) and (25), respectively, are valid beyond the first order plant in Eq. (23) and hold for all systems with one real uncancellable zero. For ZPETC and TS, the error dynamics depends on the uncancellable zero and is independent of the cancellable part of the dynamics. This dependence of ZPETC and TS error dynamics on uncancellable zero dynamics holds irrespective of the number of uncancellable zero(s). The value of J_e for FBF is independent of the uncancellable zero(s) location, whereas, for ZPETC and TS it depends on the uncancellable zero(s) location.

The J_e values for FBF, ZPETC and TS are plotted in Fig. 2 for $a \in [-10,10]$ based on parameter values $M = 1000$, $n = 990$ and $n_1 = 5$. Note that FBF is defined for all zero locations, whereas, ZPETC and TS are not applicable for $a = 1$ and $|a| = 1$, respectively. It must be pointed out that approximate inversion is not generally used for tracking control in the minimum phase (MP) region because $C = G^{-1}$ can be employed (providing a is not poorly damped [1]). However, we have included the MP region in Fig. 2 for the sake of completeness. The variation of J_e with a seen in Fig. 2 for FBF, ZPETC and TS are in agreement with observations made in the literature; i.e.:

- The FBF method demonstrates very consistent tracking performance irrespective of plant dynamics [10,11,16].
- The performance of ZPETC for left hand plane (LHP) zeros is better than that for right hand plane (LHP) zeros and the worst case is around $a = 1$ [4].
- The performance of TS for RHP and LHP zeros is the same, i.e., its performance is symmetric with respect to the imaginary axis. However, its performance degrades drastically as $|a| \to 1$ for a fixed n_1. To improve its performance as $|a| \to 1$, n_1 must approach infinity [2].

Remark 6: Note that $\mathbf{L}_{ZPETC}$ and $\mathbf{L}_{TS}$ have full rank (M+1), hence their better performance than $\mathbf{L}_{FBF}$ in Fig. 2 for some values of a; if $\mathbf{L}_{FBF}$ is allowed to achieve full rank ($n = M$) it will result in the best possible performance, i.e., perfect tracking (at least in theory). Hence, the relative accuracy between FBF and the other methods is not of particular interest, since the accuracy of FBF can always be improved by using higher n [10].

The tracking performance predictions of J_e as a function of a in Fig. 2 are validated in simulations using a zero-mean white noise signal, with variance equal to 1, M = 1000 and sampling frequency 10 kHz, as the desired trajectory (y_d). The white noise nature of the desired trajectory ensures that it has equal intensity at different frequencies. Figure 3 shows the effect of zero location a on normalized RMS tracking error $\mathbf{e}_{RMS}/\mathbf{y}_{d,RMS}$. For FBF, two rudimentary basis functions are used: (i) discrete cosine transform (DCT) [21], and (ii) block pulse functions (BPF) [23]. The DCT is a frequency-based transform that is widely used in signal processing; its basis functions are real-valued cosines defined as follows [10,21]

$$\varphi_i(k) = \beta_i \cos\left(\frac{\pi(2k+1)i}{2(M+1)}\right) \quad \beta_i = \begin{cases} \dfrac{1}{\sqrt{M+1}} & i = 0 \\ \sqrt{\dfrac{2}{M+1}} & i > 0 \end{cases} \tag{26}$$

The BPF basis functions [23] are given by

$$\varphi_i(k) = \begin{cases} 1 & k \in \left[i\dfrac{M}{n+1}, (i+1)\dfrac{M}{n+1} \right), 0 \le i < n \\ & \& \; k \in \left[i\dfrac{M}{n+1}, (i+1)\dfrac{M}{n+1} \right], i = n \\ 0 & \text{otherwise} \end{cases} \tag{27}$$

The BPF expressed in Eq. (27) seeks to divide the time interval from 0 to M among n+1 basis functions in a quasi-uniform manner. Other parameters M = 1000, n = 990 and n_1 = 5 are same as that used for generating the J_e plots in Fig. 2. Notice that the trend for J_e (Fig. 2) and $\mathbf{e}_{RMS}/\mathbf{y}_{d,RMS}$ (Fig. 3) are very similar, which indicates the effectiveness of the proposed metric as an indicator of tracking performance. It confirms that the tracking performance of FBF does not vary much with zero location and type of basis functions. However, the tracking performances of ZPETC and TS change drastically with zero location in the pattern predicted by their respective J_e values. It must be noted that there might be instances when the performance trends might not exactly follow insights drawn from the Frobenius norm metric. For example, FBF might have much better tracking performance than predicted by J_e if one purposely (or accidently) uses filtered basis functions that span the desired trajectory (y_d). But, in general, the proposed Frobenius norm metric provides good insights about tracking performance and one can expect a more consistent performance (with respect to the zero location) with FBF compared to ZPETC and TS.

Remark 7: The inconsistent performance of ZPETC and TS predicted by J_e in Fig. 2 and validated numerically in Fig. 3 is faced by most other tracking control methods [4]. Therefore, the consistent tracking performance of FBF predicted by $J_{e,FBF}$ and validated in Fig. 3, as well as in Refs. [10,11,16], sets it apart from most other tracking control methods.

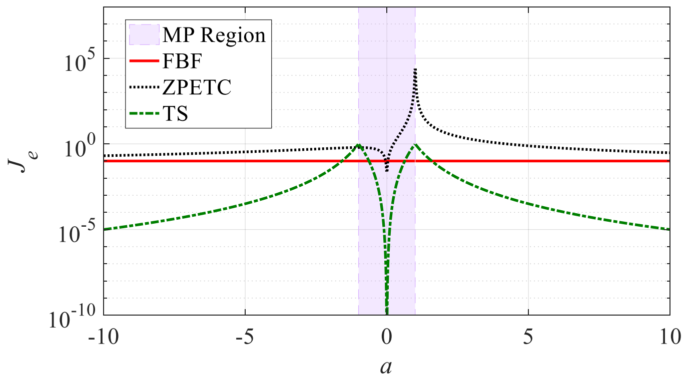

Figure 2: Effect of zero location on Frobenius norm metric for FBF, ZPETC and TS (M = 1000, n = 990, n_1 = 5). ZPETC is not applicable for a = 1 and TS is not applicable for |a| = 1. The methods are also simulated for MP region but the plant can also be inverted in this region.

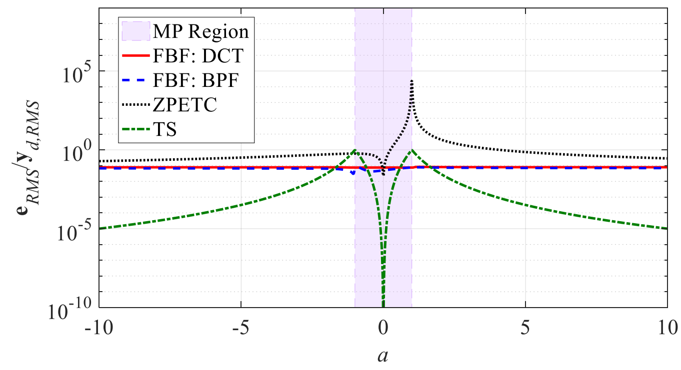

Figure 3: Effect of zero location on normalized RMS tracking error for FBF (DCT, BPF), ZPETC and TS (M = 1000, n = 990, n_1 = 5). ZPETC is not applicable for a = 1 and TS is not applicable for |a| = 1.

5. CONCLUSION

This paper proposes a metric to evaluate the tracking performance of discrete-time LTI and LTV tracking controllers using the Frobenius norm of the control system's lifted system representation. It is shown that the proposed Frobenius norm metric is closely related to the integral of the squared magnitude of the error dynamics; the metric also establishes an upper bound on tracking error.

Moreover, it is shown that the FBF approach for tracking control of LTI NMP systems (which results in an LTV controller) is the optimal solution to the rank constrained minimization of the proposed metric. It is very interesting that, for FBF, the proposed Frobenius norm metric is independent of the plant dynamics and type of basis functions, whereas, for ZPETC and TS the metric is dependent on plant dynamics (specifically, zero location). The observations made using the proposed metric regarding FBF, ZPETC and TS are in agreement with those made in the literature. Analysis and simulations based on a plant with varying zero locations are used to further confirm the effectiveness of the proposed metric as a tool for evaluating the tracking performance of LTI and LTV discrete-time controllers.

Ongoing work is focused on extending the study presented in this paper to cases involving complex NMP zeros, and extending the metric to the study of other factors of importance in tracking control, like control effort and robustness.

ACKNOWLEDGMENTS

This work is partially funded by US National Science Foundation's CAREER Award No. 1350202.

REFERENCES

[1] Tomizuka, M., 1987, "Zero Phase Error Tracking Algorithm for Digital Control," J. Dyn. Syst. Meas. Control, **109**(1), pp. 65–68.

[2] Gross, E., Tomizuka, M., and Messner, W., 1994, "Cancellation of Discrete Time Unstable Zeros by Feedforward Control," J. Dyn. Syst. Meas. Control, **116**(1), pp. 33–38.

[3] Lunenburg, J., Bosgra, O., and Oomen, T., 2009, "Inversion-Based Feedforward Design for Beyond Rigid Body Systems : A Literature Survey," DCT Rep. 2009.105, Eindhoven Univ. Technol. Eindhoven, Netherlands.

[4] Butterworth, J. A., Pao, L. Y., and Abramovitch, D. Y., 2012, "Analysis and Comparison of Three Discrete-Time Feedforward Model-Inverse Control Techniques for Nonminimum-Phase Systems," Mechatronics, **22**(5), pp. 577–587.

[5] Clayton, G. M., Tien, S., Leang, K. K., Zou, Q., and Devasia, S., 2009, "A Review of Feedforward Control Approaches in Nanopositioning for High-Speed SPM," J. Dyn. Syst. Meas. Control, **131**(6), p. 61101.

[6] Rigney, B. P., Pao, L. Y., and Lawrence, D. A., 2009, "Nonminimum Phase Dynamic Inversion for Settle Time Applications," Control Syst. Technol. IEEE Trans., **17**(5), pp. 989–1005.

[7] Bristow, D. A., Tharayil, M., and Alleyne, A. G., 2006, "A Survey of Iterative Learning Control," IEEE Control Syst. Mag., **26**(3), pp. 96–114.

[8] Hashemi, S., and Hammond, J., 1996, "The Interpretation of Singular Values in the Inversion of Minimum and Non-Minimum Phase Systems," Mech. Syst. Signal Process., **10**(3), pp. 225–240.

[9] Ronde, M., van de Molengraft, R., and Steinbuch, M., 2012, "Model-based Feedforward for Inferential Motion Systems, with Application to a Prototype Lightweight Motion System," American Control Conference (ACC), 2012, pp. 5324–5329.

[10] Ramani, K. S., Duan, M., Okwudire, C. E., and Ulsoy, A. G., 2017, "Tracking Control of Linear Time-Invariant Nonminimum Phase Systems Using Filtered Basis Functions," J. Dyn. Syst. Meas. Control. Press, **139**(1), p. 11001.

[11] Duan, M., Ramani, K. S., and Okwudire, C. E., 2015, "Tracking Control of Non-Minimum Phase Systems Using Filtered Basis Functions: A NURBS-Based Approach," ASME 2015 Dynamic Systems and Control Conference, American Society of Mechanical Engineers, p. V001T03A006--V001T03A006.

[12] Kasemsinsup, Y., Romagnoli, R., Heertjes, M., Weiland, S., and Butler, H., 2017, "Reference-tracking Feedforward Control Design for Linear Dynamical Systems through Signal Decomposition," American Control Conference (ACC), 2017, pp. 2387--2392.

[13] Frueh, J. A., and Phan, M. Q., 2000, "Linear Quadratic Optimal Learning Control (LQL)," Int. J. Control, **73**(10), pp. 832–839.

[14] van Zundert, J., Oomen, T., Goswami, D., and Heemels, W., 2016, "On the Potential of Lifted Domain Feedforward Controllers with a Periodic Sampling Sequence," American Control Conference (ACC), 2016, pp. 4227–4232.

[15] Barton, K. L., Bristow, D. A., and Alleyne, A. G., 2010, "A Numerical Method for Determining Monotonicity and Convergence Rate in Iterative Learning Control," Int. J. Control, **83**(2), pp. 219–226.

[16] Duan, M., Yoon, D., and Okwudire, C. E., 2017, "A Limited-Preview Filtered B-Spline Approach to Tracking Control – with Application to Vibration-Induced Error Compensation of a Commercial 3D Printer," Mechatronics.

[17] Eckart, C., and Young, G., 1936, "The Approximation of One Matrix by Another of Lower Rank," Psychometrika, **1**(3), pp. 211–218.

[18] Mirsky, L., 1960, "Symmetric Gauge Functions and Unitarily Invariant Norms," Q. J. Math., **11**, pp. 50–59.

[19] Markovsky, I., 2008, "Structured Low-Rank Approximation and its Applications," Automatica, **44**(4), pp. 891–909.

[20] Phan, M., and Frueh, J., 1996, "Learning Control for Trajectory Tracking using Basis Functions," Decision and Control, 1996., Proceedings of the 35th IEEE Conference on, pp. 2490–2492.

[21] Ye, Y., and Wang, D., 2005, "DCT Basis Function Learning Control," Mechatronics, IEEE/ASME Trans., **10**(4), pp. 449–454.

[22] Yoon, D., and Okwudire, C. E., 2016, "Active Assist Device for Simultaneous Reduction of Heat and Vibration in Precision Scanning Stages," Precis. Eng., **46**, pp. 193–205.

[23] Deb, A., Sarkar, G., and Sen, S. K., 1994, "Block Pulse Functions, the Most Fundamental of all Piecewise Constant Basis Functions," Int. J. Syst. Sci., **25**(2), pp.

351–363.
[24] Oppenheim, A. V, Schafer, R. W., and Buck, J. R., 1989, Discrete-time Signal Processing, Prentice-hall Englewood Cliffs.
[25] Riley, K. F., Hobson, M. P., and Bence, S. J., 2006, Mathematical Methods for Physics and Engineering: A Comprehensive Guide, Cambridge university press.

APPENDIX A: Lifted System Representation (LSR)

An LTI SISO causal plant G can be expressed as

$$G(q) = g_0 + g_1 q^{-1} + g_2 q^{-2} + \ldots \tag{28}$$

where the coefficients g_l are the Markov parameters of G. The sequence g_0, g_1, g_2, … also represent the impulse response of G. Then

$$\underbrace{\begin{bmatrix} y(0) \\ y(1) \\ \vdots \\ y(M) \end{bmatrix}}_{\mathbf{y}} = \underbrace{\begin{bmatrix} g_0 & 0 & \ldots & 0 \\ g_1 & g_0 & \ldots & 0 \\ \vdots & \vdots & \ddots & \vdots \\ g_M & g_{M-1} & \ldots & g_0 \end{bmatrix}}_{\mathbf{G}} \underbrace{\begin{bmatrix} u(0) \\ u(1) \\ \vdots \\ u(M) \end{bmatrix}}_{\mathbf{u}} \tag{29}$$

For a LTI non-causal controller C

$$C(q) = \ldots + c_{-2} q^2 + c_{-1} q^1 + c_0 + c_1 q^{-1} + c_2 q^{-2} + \ldots \tag{30}$$

the lifted system representation $\mathbf{C}$ can be expressed as

$$\underbrace{\begin{bmatrix} u(0) \\ u(1) \\ \vdots \\ u(M) \end{bmatrix}}_{\mathbf{u}} = \underbrace{\begin{bmatrix} c_0 & c_{-1} & \ldots & c_{-M} \\ c_1 & c_0 & \ldots & c_{-M+1} \\ \vdots & \vdots & \ddots & \vdots \\ c_M & c_{M-1} & \ldots & c_0 \end{bmatrix}}_{\mathbf{C}} \underbrace{\begin{bmatrix} y_d(0) \\ y_d(1) \\ \vdots \\ y_d(M) \end{bmatrix}}_{\mathbf{y}_d} \tag{31}$$

Similarly, L and E_{ff} can be expressed in lifted domain as $\mathbf{L}$ and $\mathbf{E}_{ff}$. For LTI systems, the lifted system representation is Toeplitz. For LTV systems or controllers, the construction of the lifted system representation is same but the matrix is not Toeplitz [7].

APPENDIX B: Relationship between Metric and System Dynamics 2-norm

Based on Appendix A, the squared Frobenius norm of the LSR of $E_{ff}(q)$ can be expressed as

$$\left\|\mathbf{E}_{ff}\right\|_F^2 = \sum_{l=1}^{M+1} \sum_{k=l-1-M}^{l-1} e_{ff,k}^2 \tag{32}$$

According to definition of 2-norm of $E_{ff}(q)$ and Parseval's Theorem [24]

$$\left\|E_{ff}(q)\right\|_2^2 = \frac{\int_0^{2\pi} \left|E_{ff}(e^{j\theta})\right|^2 d\theta}{2\pi} = \sum_{k=-\infty}^{\infty} e_{ff,k}^2 \tag{33}$$

where

$$E_{ff}(e^{j\theta}) = \sum_{k=-\infty}^{\infty} e_{ff,-k} e^{jk\theta} \tag{34}$$

Consider

$$(M+1)\sum_{k=-\infty}^{\infty} e_{ff,k}^2 = \sum_{l=1}^{M+1} \sum_{k=-\infty}^{\infty} e_{ff,k}^2 \tag{35}$$

and using Eq. (32)

$$\begin{aligned} (M+1)\sum_{k=-\infty}^{\infty} e_{ff,k}^2 = \left\|\mathbf{E}_{ff}\right\|_F^2 & \\ + (M+1)\sum_{k=-\infty}^{-M-1} e_{ff,k}^2 & \\ + (M+1)\sum_{k=M+1}^{\infty} e_{ff,k}^2 & \\ + \sum_{k=-M}^{M} |k| e_{ff,k}^2 & \end{aligned} \tag{36}$$

Re-arrangement of the terms in the equation results in

$$\begin{aligned} \frac{\left\|\mathbf{E}_{ff}\right\|_F^2}{M+1} = \sum_{k=-\infty}^{\infty} e_{ff,k}^2 - \sum_{k=-\infty}^{-M-1} e_{ff,k}^2 \\ - \sum_{k=M+1}^{\infty} e_{ff,k}^2 - \sum_{k=-M}^{M} \frac{|k|}{M+1} e_{ff,k}^2 \end{aligned} \tag{37}$$

Consider two different values of M, M_1 and M_2 such that $M_1 > M_2$, then

$$\begin{aligned} &\frac{\left\|\mathbf{E}_{ff}[M_1]\right\|_F^2}{M_1+1} - \frac{\left\|\mathbf{E}_{ff}[M_2]\right\|_F^2}{M_2+1} \\ &= -\sum_{k=-\infty}^{-M_1-1} e_{ff,k}^2 + \sum_{k=-\infty}^{-M_2-1} e_{ff,k}^2 - \sum_{k=M_1+1}^{\infty} e_{ff,k}^2 + \sum_{k=M_2+1}^{\infty} e_{ff,k}^2 \\ &\quad - \sum_{k=-M_1}^{M_1} \frac{|k|}{M_1+1} e_{ff,k}^2 + \sum_{k=-M_2}^{M_2} \frac{|k|}{M_2+1} e_{ff,k}^2 \\ &= \sum_{k=-M_1}^{-M_2-1} e_{ff,k}^2 + \sum_{k=M_2+1}^{M_1} e_{ff,k}^2 \\ &\quad - \sum_{k=-M_1}^{-M_2-1} \frac{|k|}{M_1+1} e_{ff,k}^2 - \sum_{k=M_2+1}^{M_1} \frac{|k|}{M_1+1} e_{ff,k}^2 \\ &\quad - \sum_{k=-M_2}^{M_2} \frac{|k|}{M_1+1} e_{ff,k}^2 + \sum_{k=-M_2}^{M_2} \frac{|k|}{M_2+1} e_{ff,k}^2 \\ &= \sum_{k=-M_1}^{-M_2-1} \left(1 - \frac{|k|}{M_1+1}\right) e_{ff,k}^2 + \sum_{k=M_2+1}^{M_1} \left(1 - \frac{|k|}{M_1+1}\right) e_{ff,k}^2 \\ &\quad + \sum_{k=-M_2}^{M_2} \left(\frac{1}{M_2+1} - \frac{1}{M_1+1}\right) |k| e_{ff,k}^2 \\ &> 0 \end{aligned} \tag{38}$$

where $\mathbf{E}_{ff}[M_1]$ and $\mathbf{E}_{ff}[M_2]$ denote the LSRs of $E_{ff}(q)$ for trajectory lengths M_1+1 and M_2+1, respectively. The implication is that for $M_1 > M_2$

$$\frac{\left\|\mathbf{E}_{ff}[M_1]\right\|_F^2}{M_1+1} > \frac{\left\|\mathbf{E}_{ff}[M_2]\right\|_F^2}{M_2+1} \tag{39}$$

i.e., the value of the proposed Frobenius norm metric J_e increases as M increases for a given dynamics $E_{ff}(q)$.

Combining Eqs. (33) and (37)

$$\frac{\left\|\mathbf{E}_{ff}\right\|_F^2}{M+1} = \left\|E_{ff}(q)\right\|_2^2 - \sum_{k=-\infty}^{-M-1} e_{ff,k}^2 - \sum_{k=M+1}^{\infty} e_{ff,k}^2 - \sum_{k=-M}^{M} \frac{|k|}{M+1} e_{ff,k}^2 \tag{40}$$

As $M\to\infty$, the first two summation terms on right hand side of Eq. (40) tend to 0. Assume that $e_{ff,k}$ is bounded by an exponential function, i.e.,

$$e_{ff,k}^2 \le A e^{-\mu|k|} \tag{41}$$

where e (on the right hand side) is the Euler's number and A and μ are positive non-zero constants. The implication of the assumption is that the output of dynamics E_{ff} at a particular instant of time depends more on input at the current time instant and inputs immediately preceding or succeeding the current input as compared to inputs which occurred long time back or will occur after a long time in the future. This assumption is true for stable systems. Hence, the third summation term on right hand side of Eq. (40) is bounded by

$$\sum_{k=-M}^{M} \frac{|k|}{M+1} e_{ff,k}^2 \le A \sum_{k=-M}^{M} \frac{|k|}{M+1} e^{-\mu|k|} \tag{42}$$

Consider the bound on the summation,

$$A \sum_{k=-M}^{M} \frac{|k|}{M+1} e^{-\mu|k|} = 2A \sum_{k=0}^{M} \frac{k}{M+1} e^{-\mu k} \tag{43}$$

The summation on the right hand side represents summation of an arithmetico-geometric sequence [25]. As $M\to\infty$ (based on sum of infinite arithmetico-geometric sequence with absolute value of common ratio of the geometric part of the sequence bounded by 1, i.e., $|e^{-\mu}| < 1$)

$$\begin{aligned} &\lim_{M\to\infty} 2A \sum_{k=0}^{M} \frac{k}{M+1} e^{-\mu k} \\ &= \lim_{M\to\infty} 2A \frac{1}{M+1} \frac{e^{-\mu}}{(1-e^{-\mu})^2} = 0 \end{aligned} \tag{44}$$

which implies that

$$\begin{aligned} &\lim_{M\to\infty} \sum_{k=-M}^{M} \frac{|k|}{M+1} e_{ff,k}^2 \\ &\le \lim_{M\to\infty} A \sum_{k=-M}^{M} \frac{|k|}{M+1} e^{-\mu|k|} = 0 \end{aligned} \tag{45}$$

The implication is that (based on Eqs. (40) and (45))

$$J_e = \frac{\left\|\mathbf{E}_{ff}\right\|_F}{\sqrt{M+1}} \to \left\|E_{ff}(q)\right\|_2 \quad \text{as } M\to\infty \tag{46}$$

APPENDIX C: Eckart-Young-Mirsky (EYM) Theorem [17–19]

Consider matrix $\mathbf{A}$ ($r_1 \times r_2$, $r_1 \le r_2$) and $0 < r < r_1$, r is an integer, SVD of $\mathbf{A}$ (assuming full rank) is given by

$$\mathbf{A} = \sum_{i=1}^{r_1} \sigma_{A,i} \mathbf{v}_{A,i} \mathbf{w}_{A,i}^{\mathrm{T}} \tag{47}$$

then solution to the following problem

$$\hat{\mathbf{A}}^* := \arg\min_{\hat{\mathbf{A}}} \left\|\mathbf{A} - \hat{\mathbf{A}}\right\|_F \quad \text{s.t. } rank(\hat{\mathbf{A}}) \le r \tag{48}$$

is given by

$$\hat{\mathbf{A}}^* = \sum_{i=1}^{r} \sigma_{A,i} \mathbf{v}_{A,i} \mathbf{w}_{A,i}^{\mathrm{T}} \tag{49}$$

i.e., a truncated singular value decomposition and

$$\left\|\mathbf{A} - \hat{\mathbf{A}}^*\right\|_F = \sqrt{\sum_{i=r+1}^{r_1} \sigma_{A,i}^2} \tag{50}$$

The solution is unique if and only if $\sigma_{A,r+1} \ne \sigma_{A,r}$.

Consider the rank constrained optimization problem

$$\min_{\mathbf{L}} \left\{ J_e = \frac{\left\|\mathbf{I} - \mathbf{L}\right\|_F}{\sqrt{M+1}} \right\} \quad \text{s.t. } rank(\mathbf{L}) \le n+1 \tag{51}$$

The SVD of $\mathbf{I}$ is of the form (the SVD is not unique)

$$\mathbf{I} = \sum_{i=1}^{M+1} \boldsymbol{\eta}_i \boldsymbol{\eta}_i^{\mathrm{T}} \tag{52}$$

where

$$\boldsymbol{\eta}_i^{\mathrm{T}} \boldsymbol{\eta}_j = \delta_{ij}, \qquad \delta_{ij} = \begin{cases} 1 & i = j \\ 0 & i \ne j \end{cases} \tag{53}$$

For constant M, based on the EYM Theorem, one can conclude that the optimal solution is not unique and is of the form

$$\mathbf{L}_{opt} = \sum_{i=1}^{n+1} \boldsymbol{\eta}_i \boldsymbol{\eta}_i^{\mathrm{T}} \tag{54}$$

From prior work [10] and Sec. 3.1, it is known that the lifted system representation of FBF overall dynamics, which will vary depending on the selected basis functions and the plant, is

$$\mathbf{L}_{FBF} = \tilde{\boldsymbol{\Psi}} \tilde{\boldsymbol{\Psi}}^{\mathrm{T}} = \sum_{i=1}^{n+1} \tilde{\boldsymbol{\psi}}_i \tilde{\boldsymbol{\psi}}_i^{\mathrm{T}} \tag{55}$$

where $\tilde{\boldsymbol{\psi}}_i$ are the columns of $\tilde{\boldsymbol{\Psi}}$

$$\tilde{\boldsymbol{\psi}}_i^{\mathrm{T}} \tilde{\boldsymbol{\psi}}_j = \delta_{ij} \tag{56}$$

Every optimal solution of Eq. (51) is given by Eqs. (53) and (54) and every FBF overall dynamics can be expressed using Eqs. (55) and (56). Based on Eqs. (53)-(56) one can conclude that every optimal solution of Eq. (51) represents an FBF overall dynamics and every FBF overall dynamics is an optimal solution of Eq. (51).